Analyst

Cite this: *Analyst*, 2011, **136**, 2106

www.rsc.org/analyst

PAPER

A novel fluorescent biosensor for sequence-specific recognition of double-stranded DNA with the platform of graphene oxide

Chengke Wu,[a] Yamin Zhou,[b] Xiangmin Miao[a] and Liansheng Ling*[a]

Received 24th January 2011, Accepted 1st March 2011
DOI: 10.1039/c1an15061h

A fluorescent biosensor for sequence-specific recognition of double-stranded DNA (dsDNA) was developed based upon the DNA hybridization between dye-labeled single-stranded DNA (ssDNA) and double-stranded DNA. The fluorescence of FAM-labeled single-stranded DNA was quenched when it adsorbed on the surface of graphene oxide (GO). Upon addition of the target dsDNA, a homopyrimidine·homopurine part of dsDNA on the Simian virus 40 (SV40) (4424–4440, gp6), hybridization occurred between the dye-labeled DNA and the target dsDNA, which induced the dye-labeled DNA desorbed from the surface of GO, and turned on the fluorescence of the dye. Under the optimum conditions, the enhanced fluorescence intensity was proportional to the concentration of target dsDNA in the range 40.0–260 nM, and the detection limit was found to be 14.3 nM alongside the good sequence selectivity.

Introduction

Graphene oxide (GO) is a derivative of graphene, and it has good water solubility compared to that of graphene.[1,2] Because of its remarkable electronic, mechanical and thermal properties, applications of GO in biology have attracted much attention recently.[3,4] Fluorescent dye-labeled single-stranded DNA (ssDNA) could adsorb on the surface of GO, accompanied with the quenching of the dye fluorescence. Whereas it desorbed from the surface of GO when hybridized with its complementary strand, and the fluorescence of the dye was recovered.[5] Because of this reason, GO was used as a platform to develop biosensors for DNA,[5,6] Hg^{2+},[6] Ag^{+},[7] proteins[8] and other molecules.[9]

Classical methods for sequence-specific recognition of DNA were based upon the DNA hybridization between two complementary single-stranded DNAs, which required denaturing dsDNA prior to the research.[10] However, dsDNA is the natural structure of genome, so sequence-specific recognition of dsDNA may be used to recognize the genome of a virus directly. Therefore, sequence-specific recognition of dsDNA has drawn much attention in the last decades. For instance, polyamides[11,12] and zinc finger DNA-binding protein[13,14] have been applied to recognize dsDNA successively. Moreover, homopyrimidine·homopurine dsDNA could be recognized with oligonucelotide based upon the formation of triplex DNA through Hoogsteen hydrogen bonding or anti-Hoogsteen hydrogen bonding. Therefore, some genomes containing the homopyrimidine·homopurine duplex structure can be recognized by specific oligonucleotide through triplex formation.[15–20]

Simian virus 40 (SV40) is a simple DNA-virus, a member of the Polyomaviridae family belonging to the Papovaviridae family. The SV40 T-antigen can bind with a tumor suppressor protein and make it inactive, eliminating its cytostatic function, increasing the number of cells growing in the G1-S period, accelerating the cell division, and inducing the formation of a tumor.[21,22] For these above mentioned reasons, SV40 was often served as a model for tumorigenic and anti-tumor immunity research.[23–25] Moreover, the DNA sequence at the position of 4424–4440 gp6 of SV40 is composed of homopyrimidine·homopurine dsDNA with a length of 17 base pairs, which might easily be recognized by oligonucleotide through triplex formation. Here, we developed a fluorescent method for the recognition of the homopyrimidine·homopurine part of SV40 with the platform of GO.

Experimental

Instruments and materials

Oligonucleotides were synthesized by Shanghai Sangon Biological Engineering Technology & Services Co., Ltd. (Shanghai, China). All reagents were of analytical grade without specified otherwise, and ultrapure water was used throughout the research.

Target dsDNA was composed of two complementary sequences, T1 and T2, which was the homopyrimidine·homopurine sequence located in the T antigen gene of SV40 DNA (Table 1). FAM-modified oligonucleotide (P1) was designed for recognizing the target dsDNA, which was based

[a]*School of Chemistry and Chemical Engineering, Sun Yat-Sen University, Guangzhou 510275, P.R. China. E-mail: cesllsh@mail.sysu.edu.cn; Fax: +86-20-84112245; Tel: +86-20-84110156*
[b]*College of Chemistry and Environmental Engineering, Dongguan University of Technology, Dongguan 523808, P.R. China*

Table 1 Sequence of oligonucleotides

Name	Sequence	
Probe DNA 1	5′-TTTTTTCTTCTCTTTCC-FAM-3′	P1
Target DNA	5′-AAAAAAGAAGAGAAAGG-3′	T1
	3′-TTTTTTCTTCTCTTTCC-5′	T2
One base pair replaced dsDNA (R1)	5′-AAAAAAGAGGAGAAAGG-3′	R11
	3′-TTTTTTCTCCTCTTTCC-5′	R12
Two base pair replaced dsDNA (R2)	5′-AAAAAGGAAGAAAAAGG-3′	R21
	3′-TTTTTCCTTCTTTTTCC-5′	R22

upon the triplex formation between P1 and target dsDNA by forming C^+GC and TAT triads. R1 contained two complementary sequences R11 and R12, one base pair was replaced compared to that of target dsDNA, and one mismatched triad occurred when it hybridized with P1. R2 contained two complementary sequences R21 and R22, two base pairs were replaced compared to that of target dsDNA, thereby two mismatched triads existed when it hybridized with P1.

Synthesis of graphene oxide

Graphene oxide (GO) was prepared from graphite powder according to Hummers' methods.[26] Graphite powder (1.0 g, 325 mesh) was put into cold sulfuric acid (23.0 mL, 0 °C). Then 3.0 g $KMnO_4$ was added gingerly under stirring. The temperature was kept below 20 °C by using a ice-bath during the process of adding the $KMnO_4$. After addition of $KMnO_4$, the ice-bath was removed and the suspension was stirred at 35 °C for 30 min. Afterwards, 46.0 mL ultrapure water was added slowly, and the temperature of the suspension was increased to 98 °C and kept for 15 min, then the suspension was further diluted to 140 mL with warm ultrapure water (40 °C) and treated with H_2O_2 (1.0 mL, 30%); the color of the suspension changed from black to yellow. Then the yellow suspension was separated by centrifugation and washed repeatedly with HCl (1 : 10). The final product was dried at 60 °C for three days. The product was characterized with a D-MAX 2200 X-ray diffractometer (Rigaku Corporation, Japan). As shown in Fig. 1, it had a peak at $2\theta = 11.3°$, and there was no peak at $2\theta = 26.4°$ for graphite, which was the same as that reported previously.[27]

Scanning electron micrographs of graphene oxide were obtained using a JSF-6330F Field Emission Scanning Electron Microscope (JEOL Ltd., Japan). Graphene oxide was dispersed by ultrasonic method in water and dropped onto a sample copper stage. Then the sample was dried using an infrared lamp. It was demonstrated in Fig. 2 that graphene oxide had an uneven surface and ladder-like edge. It indicated that the thickness of the GO was about 2.0 nm.

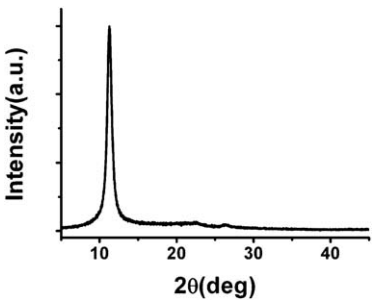

Fig. 1 XRD spectrum of graphene oxide.

Fluorescence assay for DNA

In a typical measurement, P1 (10 μM, 10 μL) with different concentrations of target dsDNA was added to graphene oxide (1 mg mL^{-1}, 10 μL). Then the mixture was diluted to 1000 μL with PBS buffer solution (10 mM, pH 6.5, 100 mM NaCl), and the fluorescence was measured using an RF-5301PC spectrofluorimeter (Shimadzu, Japan) with an IR sensitive detector. The fluorescence intensity was obtained from the emission spectrum at the wavelength of 520 nm, the excitation wavelength was set at 480 nm. The slit widths for excitation and emission were both set at 10 nm.

Circular dichroism spectra for DNA

The circular dichroism (CD) spectra were recorded with a J-810 Circular Dichroism spectrometer (JASCO International CO. Ltd., Japan). The volume of optical chamber was 400 μL, and the path length was 1.0 mm. The background of the buffer solution was subtracted from the CD data.

Results and discussions

Characteristic of spectra

Fig. 3 demonstrated the scheme of specific recognition of dsDNA with dye-modified oligonucleotide using the platform of GO. Single-stranded oligonucleotide had soft structure, and could adsorb on the surface of GO, which brought the fluorescent dye

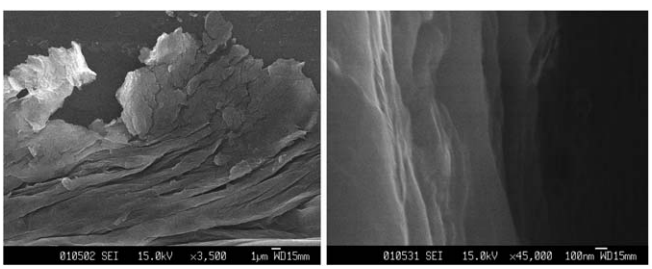

Fig. 2 Scanning electron micrographs of graphene oxide. The left image is the uneven surface topography of GO, and the right image is the ladder-like edge topography of GO.

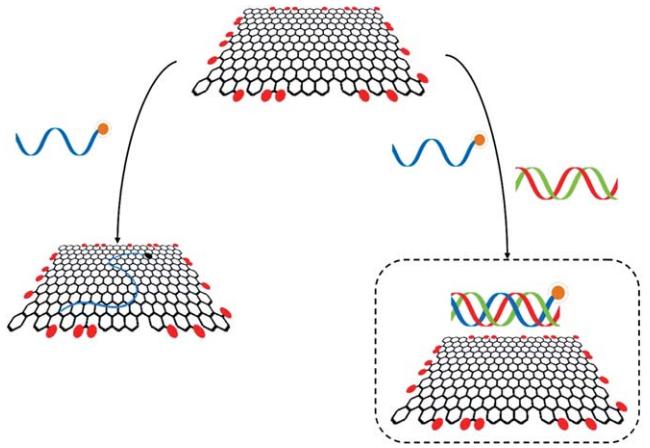

Fig. 3 Scheme of specific recognition of dsDNA with dye-modified oligonucleotide and the platform of GO. Dye-labeled oligonucleotide adsorbed on the surface of GO and fluorescence of the dye was quenched (left). Dye-modified oligonucleotide hybridized with the target dsDNA and formed triplex DNA, which made it difficult to adsorb on the surface GO (right).

at the end of the oligonucleotide close to the GO, and the fluorescence of the dye was quenched by GO through fluorescence resonance energy transfer. The addition of target dsDNA could bind to the dye-modified oligonucleotide and induced the formation of triplex DNA, which had a rigid DNA backbone and could not adsorb on the surface of GO. Therefore, the mixture of dye-modified oligonucleotide and GO had strong fluorescence in the presence of target dsDNA.

This can be confirmed by the change in the fluorescence spectrum. Fig. 4a shows the fluorescence emission spectra of P1 under different conditions. In the absence of GO, P1 had a strong emission at the peak of 520 nm, but the emission was quenched in the presence of GO. However, the emission of P1 was recovered partly upon addition of target dsDNA. To illuminate the mechanism for turning on the fluorescence of P1 by target dsDNA, the CD spectrum was studied. As shown in Fig. 4b, P1 had a weak negative Cotton effect at 247 nm, and this may due to its soft structure. Whereas target dsDNA exhibited a strong positive Cotton effect at 276 nm corresponding to base stacking, and a strong negative Cotton effect of DNA helicity around 247 nm was observed. Both the positive peak at 276 nm and the negative peak at 247 nm were relatively enhanced when P1 was mixed with target dsDNA. Moreover, a negative ellipticity peak appeared at 210 nm, which was the indicator for the structure of triplex DNA.[28] These results revealed that triplex formation occurred between P1 and target dsDNA.

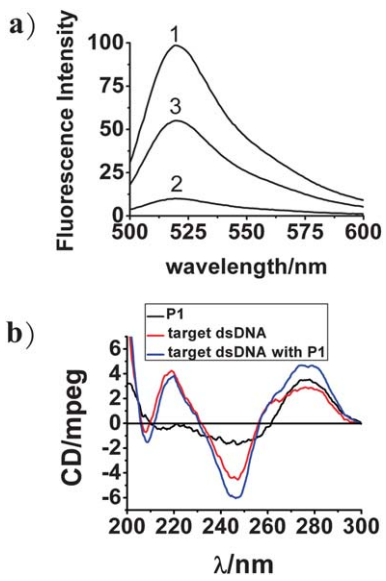

Fig. 4 (a) The fluorescence spectrum of P1 under different conditions: (1) 100 nM P1; (2) 100 nM P1 + 10 μg mL^{-1} GO; (3) 100 nM P1 + 10 μg mL^{-1} GO + 250 nM target dsDNA. pH 6.5; spermine, 0.1 μM; hybridization time, 10 min. (b) CD spectrum of the fluorescent nanoprobe without and with target dsDNA. Conditions: 10 μM P1, 10 μM dsDNA, pH 6.5, 10 μM spermine, 10 min for hybridization.

Optimization of the experimental conditions

The recognition not only depended on the sequence of the nanoprobe, but was also affected by experimental conditions. The recognition process included two steps: the first step was the triplex formation between P1 and target dsDNA; and the second step was that the probe DNA desorbed from the surface of the GO. Thus any factors that related to the above two steps can affect the recognition behavior. Therefore, experimental conditions such as pH, concentration of GO, concentration of spermine and hybridization time for the recognition were studied.

The pH environment could affect the fluorescence of the nanoprobe, the stability of triplex DNA and the adsorption property of the nanoprobe, and thus it was important to study the effect of the pH value. The effect of pH was studied over the range 4.0–10.0. As shown in Fig. 5, ΔI was increased slowly in the pH range of 4.0–6.0, increased dramatically and reached the maximum within the pH range 6.0–7.0, and then decreased with an increase of pH over the range 7.0–10.0. This may due to the protonation requirement for formation of triplex DNA and that the GO had different adsorption properties for ssDNA under the different pH environment. The adsorption ability of ssDNA on the surface of graphene oxide decreased with the increase of pH value. Moreover, the C base can be protonated under acidic medium, which is necessary for the formation of stable $C^{+}GC$ triads. However, it is difficult to protonate the C base in neutral

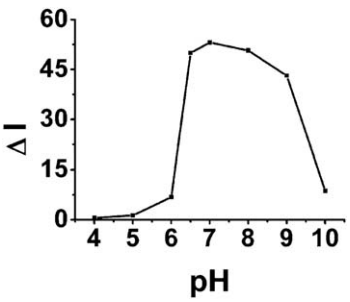

Fig. 5 Effect of pH value on the differential of fluorescence intensity (ΔI) for the mixture of P1 and GO. 100 nM P1, 250 nM target dsDNA, 10 μg mL^{-1} GO, 0.1 μM spermine, 10 min for hybridization.

or alkaline medium. Therefore, pH 6.5 buffer was chosen for controlling the pH value.

Effect of the concentration of GO was studied over the range 3.0–21.0 μg mL^{-1} (Fig. 6). When the concentration of GO was less than 7.0 μg mL^{-1}, P1 could not adsorb on the surface of GO completely, which induced the strong background, and the ΔI was weak as a result, thus the ΔI increased with the GO concentration over the range 3.0–7.0 μg mL^{-1}. It reached a plateau during the concentration range 7.0–12.0 μg mL^{-1}, which indicated that P1 was adsorbed on the surface of GO completely. An excess amount of GO was unfavorable for desorption of P1 from it through triplex formation, and ΔI decreased dramatically with the increase of GO when the concentration was higher than 12.0 μg mL^{-1}. Therefore, 10.0 μg mL^{-1} GO was used for the research.

To stabilize the structure of the triplex, multivalent cations such as Mg^{2+} and polyamines were used to neutralize the repulsion force between negatively charged ssDNA and dsDNA.[29,30] Here spermine ($H_2N(CH_2)_3NH(CH_2)_4NH(CH_2)_3NH_2$) was selected to stabilize the triplex DNA and the effect of its concentration was studied (Fig. 7). ΔI increased with the spermine concentration over the range 0–0.06 μM, it kept at a plateau over the range 0.06–0.18 μM. To obtain a stable signal, 0.1 μM spermine was used for our research. Moreover, 8.0 min was necessary for the hybridization (data not shown), and thereby 10 min was selected for the hybridization.

Under the optimum conditions, triplex formation occurred between P1 and target dsDNA accompanied with the addition of target dsDNA, which triggered the desorption of P1 from the surface of GO, and thus turned on the emission of P1. As shown in Fig. 8, the enhanced fluorescence intensity was proportional to the concentration of target dsDNA over the range 40.0–260 nM, where the regression equation was $\Delta I = 0.173C + 1.85$ (C: nM), with the correlation coefficient of 0.9970 and a detection limit of 14.3 nM ($C_{DL} = 3\delta$/slope). The relative standard deviation was 1.13% for 200 nM target dsDNA.

Sequence selectivity of the assay

The recognition of dsDNA was based upon the formation of parallel triplex DNA between P1 and the homopyrimidine·homopurine duplex strand (4424–4440 gp6) of SV40 through the formation of C^+GC and TAT triads, where GC base pair was recognized by the C base and formed C^+GC triad, while the AT base pair was recognized by the T base and formed the TAT triad. To study the sequence selectivity of the method, another two complementary duplex strands were designed for the research, compared to the target DNA, one AT base pair was replaced with GC in R1, and two base pairs were replaced in R2. As shown in Fig. 9a, the ΔI for target DNA was 50.75, while it was only 32.27 for R1, and 19.74 for R2. These results indicated the good DNA sequence selectivity of the assay, the decrease of ΔI for R1 due to the existence of one unstable TGC triad in the recognition behavior, and there were two unstable TGC and CAT triads for R2 in the recognition process, which induced the ΔI to decrease more manifestly than that of R1. The existence of the unstable triad decreased the stability of the triplex DNA, which was confirmed by CD spectrum measurements (Fig. 9b), where the negative Cotton effect at 210 nm was strong for the target dsDNA, whereas it declined dramatically for R1, and there was no negative peak at 210 nm for R2. These CD spectrum results were in good accordance with the fluorescence results of good sequence selectivity.

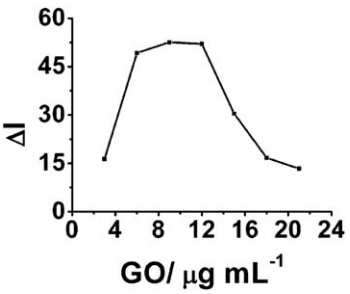

Fig. 6 Effect of the GO concentration on the differential of fluorescence intensity (ΔI) for the mixture of P1 and GO. 100 nM P1, 250 nM target dsDNA, 0.1 μM spermine, pH 6.5, 10 min for hybridization.

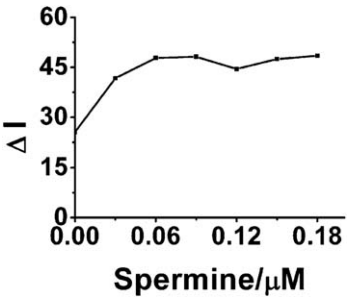

Fig. 7 Effect of the concentration of spermine on fluorescence intensity differentials (ΔI) for the mixture of P1 and GO. 100 nM P1, 250 nM target dsDNA, 10 μg mL^{-1} GO, pH 6.5, 10 min for hybridization.

Conclusions

In general, we developed a fluorescent nanoprobe for recognizing dsDNA through triplex formation with the platform of graphene oxide. The fluorescence of P1 was quenched by graphene oxide

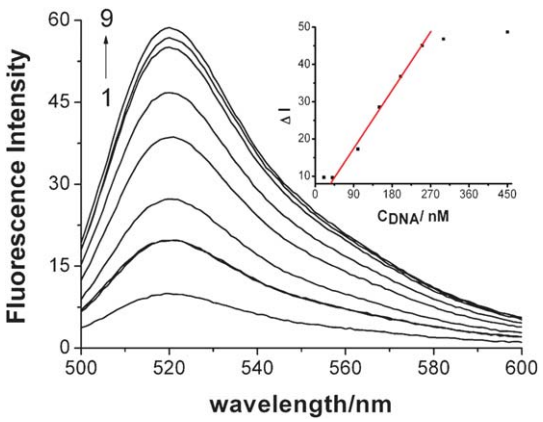

Fig. 8 The fluorescence spectrum of P1 under their optimum conditions. 100 nM P1, target dsDNA: (1) 0 nM; (2) 20 nM; (3) 40 nM; (4) 100 nM; (5) 150 nM; (6) 200 nM; (7) 250 nM; (8) 300 nM; (9) 450 nM. pH 6.5; GO, 10 μg mL^{-1}; spermine, 0.1 μM; hybridization time, 10 min.

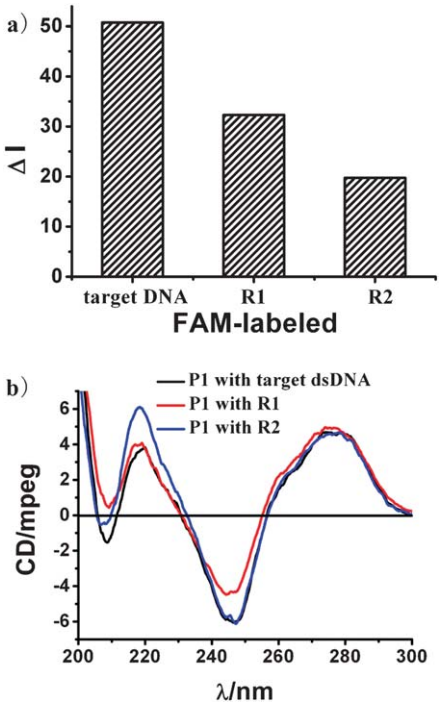

Fig. 9 Sequence selectivity of the assay. (a) P1 100 nM, target dsDNA 250 nM, R1 250 nM, R2 250 nM, GO 10 μg mL^{-1}, spermine 0.1 μM, hybridization time 10 min. (b) The CD spectrum of the fluorescent nanoprobe in the presence of different dsDNA. Conditions: 10 μM P1 with 10 μM target dsDNA (black), 10 μM P1 with 10 μM R1 (red), 10 μM P1 with 10 μM R2 (blue), pH 6.5, spermine 10 μM, hybridization time 10 min.

through fluorescence resonance energy transfer, the addition of target dsDNA resulted in the formation of triplex DNA, induced the conformation of P1 change from a coiled single strand to a rigid triplex structure, and desorbed from the surface of the graphene oxide, and turned on the fluorescence of the dye. The fluorescence enhancement was proportional to the concentration of the target dsDNA over the range of 40.0–260 nM, with a detection limit of 14.3 nM. Moreover, the sequence at the position of 4424–4440 gp6 of SV40 was the same with that of target dsDNA. Good sequence selectivity made it become a competitive method for recognizing SV40 directly. This assay provided a low-cost, rapid and sequence-specific method for recognizing dsDNA in its natural state, and diagnosing genetic and pathogenic diseases in the future.

Acknowledgements

This work was supported by the National Natural Science Foundation of China (No. 20975116).

References

1 D. Li, M. B. Muller, S. Gilje, R. B. Kaner and G. G. Wallace, *Nat. Nanotechnol.*, 2008, **3**, 101.
2 S. Stankovich, D. A. Dikin, G. H. B. Dommett, K. M. kohlhaas, E. J. Zimney, E. A. Stach, R. D. Piner, S. T. Nguyen and R. S. Ruoff, *Nature*, 2006, **442**, 282.
3 M. Nihar and B. Vikas, *Nano Lett.*, 2008, **8**, 4469.
4 D. A. Dikin, S. Stankovich, E. J. Zimney, R. D. Piner, G. H. B. Dommett, G. Evmenenko, S. T. Nguyen and R. S. Ruoff, *Nature*, 2007, **448**, 457.
5 C. H. Lu, H. H. Yang, C. L. Zhu, X. Chen and G. N. Chen, *Angew. Chem., Int. Ed.*, 2009, **48**, 4785.
6 S. J. He, B. Song, D. Li, C. F. Zhu, W. P. Qi, Y. Q. Wen, L. H. Wang, S. P. Song, H. P. Fang and C. H. Fan, *Adv. Funct. Mater.*, 2010, **20**, 453.
7 Y. Q. Wen, F. F. Xing, S. J. He, S. P. Song, L. H. Wang, Y. T. Long, D. Li and C. H. Fan, *Chem. Commun.*, 2010, **46**, 2596.
8 X. L. Zuo, S. J. He, D. Li, C. Peng, Q. Huang, S. P. Song and C. H. Fan, *Langmuir*, 2010, **26**, 1936.
9 M. Zhou, Y. M. Zhai and S. J. Dong, *Anal. Chem.*, 2009, **81**, 5603.
10 F. McKenzie, K. Faulds and D. Graham, *Chem. Commun.*, 2008, 2367.
11 P. B. Dervan and R. W. BuÈrli, *Curr. Opin. Chem. Biol.*, 1999, **3**, 688.
12 J. Fujimoto, T. Bando, P. Langer and K. Weisz, *Bioorganic & Medicinal Chemistry*, 2008, **16**, 5899.
13 M. Thompson, *Bioconjugate Chem.*, 2006, **17**, 507.
14 T. L. Roberts, A. J. Idris, A. Dunn, G. M. Kelly, C. M. Burnton, S. Hodgson, L. L. Hardy, V. Garceau, M. J. Sweet, I. L. Ross, D. A. Hume and K. J. Stacey, *Science*, 2009, **323**, 1057.
15 T. L. Doan, L. Perrouault, D. Praseuth, D. Praseuth, N. Habhoub, J. L. Decout, N. T. Thuong, J. Lhomme and C. Hélène, *Nucleic Acids Res.*, 1987, **15**, 7749.
16 B. L. Renard, R. Lartia and U. Asseline, *Org. Biomol. Chem.*, 2008, **6**, 4413.
17 S. P. Sau, P. Kumar, B. A. Anderson, M. E. Tergaard, L. Deobald, A. Paszczynski, P. K. Sharmab and P. J. Hrdlicka, *Chem. Commun.*, 2009, **44**, 6756.
18 A. Eick, Z. Xiao, P. Langer and K. Weisz, *Bioorg. Med. Chem.*, 2008, **16**, 9106.
19 P. E. Nielsen, *Curr. Opin. Mol. Ther.*, 2010, **12**, 184.
20 K. Kaihatsu, R. Shah, H. X. Zhao and D. R. Corey, *Biochemistry*, 2003, **42**, 13996.
21 S. H. Ali and J. A. DeCaprio, *Seminars in Cancer Biology*, 2001, **11**, 15.
22 D. Ahuja, M. T. Saenz-Robles and J. M. Pipas, *Oncogene*, 2005, **24**, 7729.
23 R. M. Li, M. H. Branton, S. Tanawattanacharoen, R. A. Falk, J. C. Jennette and J. B. Kopp, *J. Am. Soc. Nephrol.*, 2002, **13**, 2320.
24 R. A. Foddis, D. Rienzo, D. Broccoli, M. Bocchetta, E. Stekala, P. Rizzo, A. Tosolini, J. V. Grobelny, S. C. Jhanwar, H. I. Pass, J. R. Testa and M. Carbone, *Oncogene*, 2002, **21**, 1434.
25 L. Pelkmans, D. Puntener and A. Helenius, *Science*, 2002, **296**, 535.
26 W. S. Hummers and R. E. Offeman, *J. Am. Chem. Soc.*, 1958, **80**, 1339.
27 Y. X. Xu, H. Bai, G. W. Lu, C. Li and G. Q. Shi, *J. Am. Chem. Soc.*, 2008, **130**, 5856.
28 A. M. Soto, J. Loo and L. A. Marky, *J. Am. Chem. Soc.*, 2002, **124**, 14355.
29 L. S. Ling, H. J. Butt and R. Berger, *J. Am. Chem. Soc.*, 2004, **126**, 13992.
30 H. L. Yan, C. Xiong, H. Yuan, Z. X. Zeng and L. S. Ling, *J. Phys. Chem. C*, 2009, **113**, 17326.

